

Supplemental material

The dynamic driving mechanisms of wetland change from an asynchrony-spatiotemporal perspective: A a case study in Pearl River Delta, China

Xiaoqing Yi^{a,b,1}, Yuhang Wang^{c,1,*}, Changjun Gao^{a,b,*}, Jiaojiao Ma^{a,b}, Demin Zhou^c, Christian J.

Sanders^d, Guangjia Jiang^e, Zhongwen Hu^f, Junjie Wang^g, Haichao Zhou^g, Wei Li^h

^a Guangdong Provincial Key Laboratory of Silviculture, Protection and Utilization, Guangdong Academy of Forestry, Guangzhou 510520, China

^b Guangdong Haifeng Wetland Ecosystem National Observation and Research Station, Guangzhou 510520, China

^c College of Resource Environment and Tourism, Capital Normal University, Beijing, 100048, China

^d National Marine Science Centre, School of Environment, Science and Engineering, Southern Cross University, Coffs Harbour NSW 2450, Australia

^e South China Sea Environment Monitoring Center, State Oceanic Administration, Guangzhou 510300, China

^f MNR Key Laboratory for Geo-Environmental Monitoring of Great Bay Area, Shenzhen University, Shenzhen 518060, China

^g College of Life Science and Oceanography, Shenzhen University, Shenzhen 518060, China

^h Institute of Wetland Research, Chinese Academy of Forestry, Beijing 100091, China

¹ These authors contribute equally to this work.

***Corresponding author:**

Yuhang Wang

Postal address: College of Resource Environment and Tourism, Capital Normal University, Beijing, 100048, China

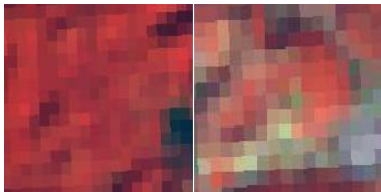
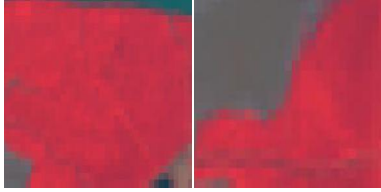
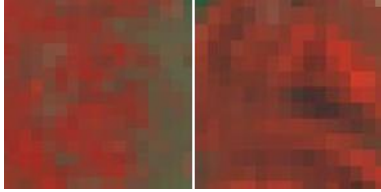
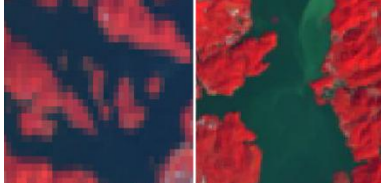
Email: yuhangww@gmail.com; 2220902167@cnu.edu.cn; Tel: +86-19828168033

Changjun Gao

Postal address: Guangdong Provincial Key Laboratory of Silviculture, Protection and Utilization, Guangdong Academy of Forestry, Guangzhou 510520, China; Guangdong Haifeng Wetland Ecosystem National Observation and Research Station, Guangzhou 510520, China

Email: gaochangjun@sinogaf.cn; gaochangjun015@163.com

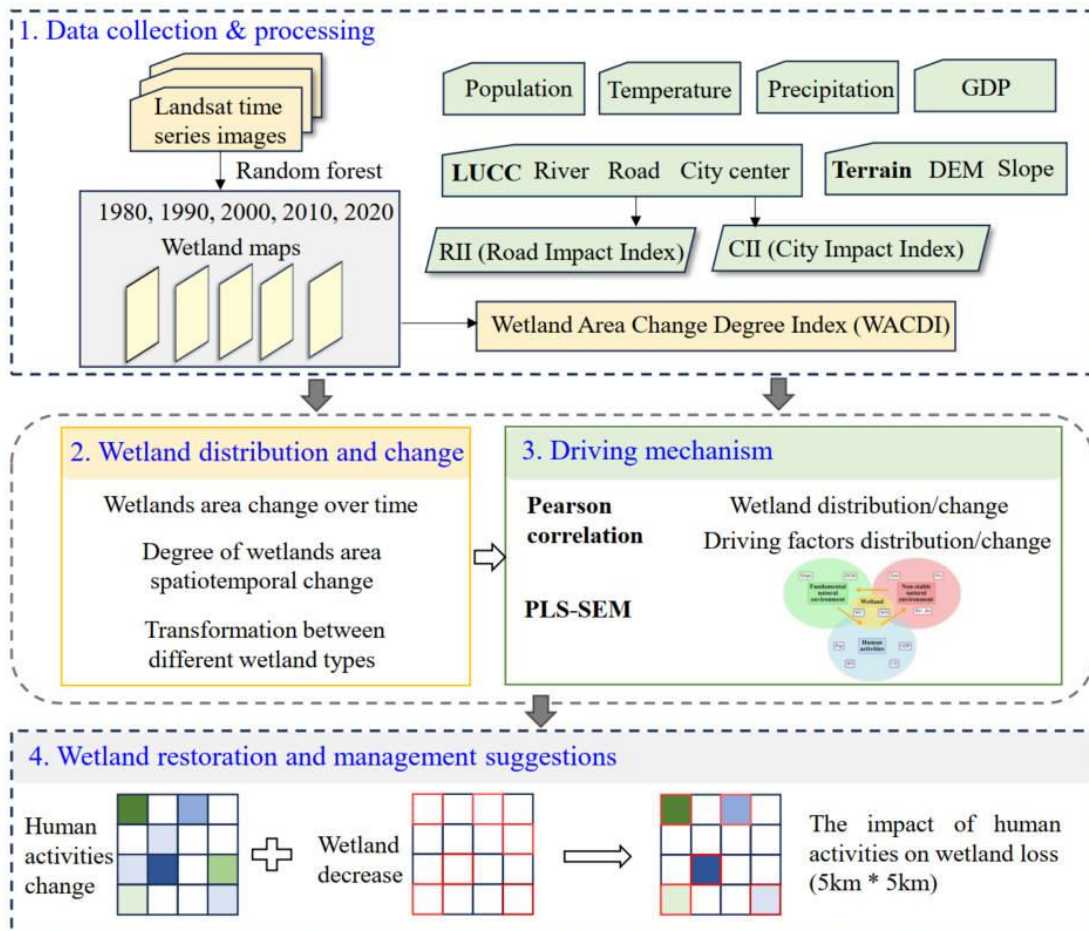
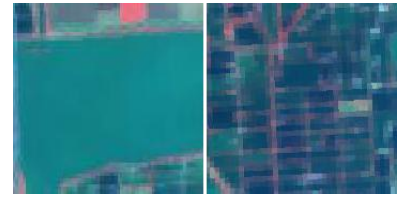
Table S1. Wetland satellite remote sensing interpretation indicators based on Landsat series data

| Weland type | Characteristics | Standard false color image |
|-------------------|---|---|
| Marsh | It is Dark red and light red patches with dark patches of water, and large bodies of water such as lakes and rivers often appear in the adjacent area. The texture is relatively rough and the color gamut is uneven. |  |
| Forested wetlands | It is dark red with dark black stripes or spots. The texture is relatively smooth and the shape is relatively regular. It is mainly distributed in the coastal zone mudflat area, and mainly mangroves. |  |
| Shrub swamps | It is dark red in color. The shape is relatively irregular, and the texture is also rough, with obvious granular shape. |  |
| Lake | It is brown in color, with smooth texture and natural boundaries. |  |

Reservoir and ponds
 Mainly including artificially excavated water bodies or artificially managed drinking water sources areas. The texture of excavated water bodies is relatively rough, with darker colors and obvious regular patches. The artificially managed drinking water sources areas has a smooth texture, but the surrounding boundaries are relatively regular.

River
 Including rivers, beaches and mudflat. The texture is relatively smooth. The water color is dark blue, and the beach and mudflat are dark gray with scattered red spots.

Paddy field
 The color is pale and accompanied by small brown patches. The texture is relatively rough and has a regular grid like pattern. Distributed in areas with abundant water sources such as rivers, reservoirs, and ponds.



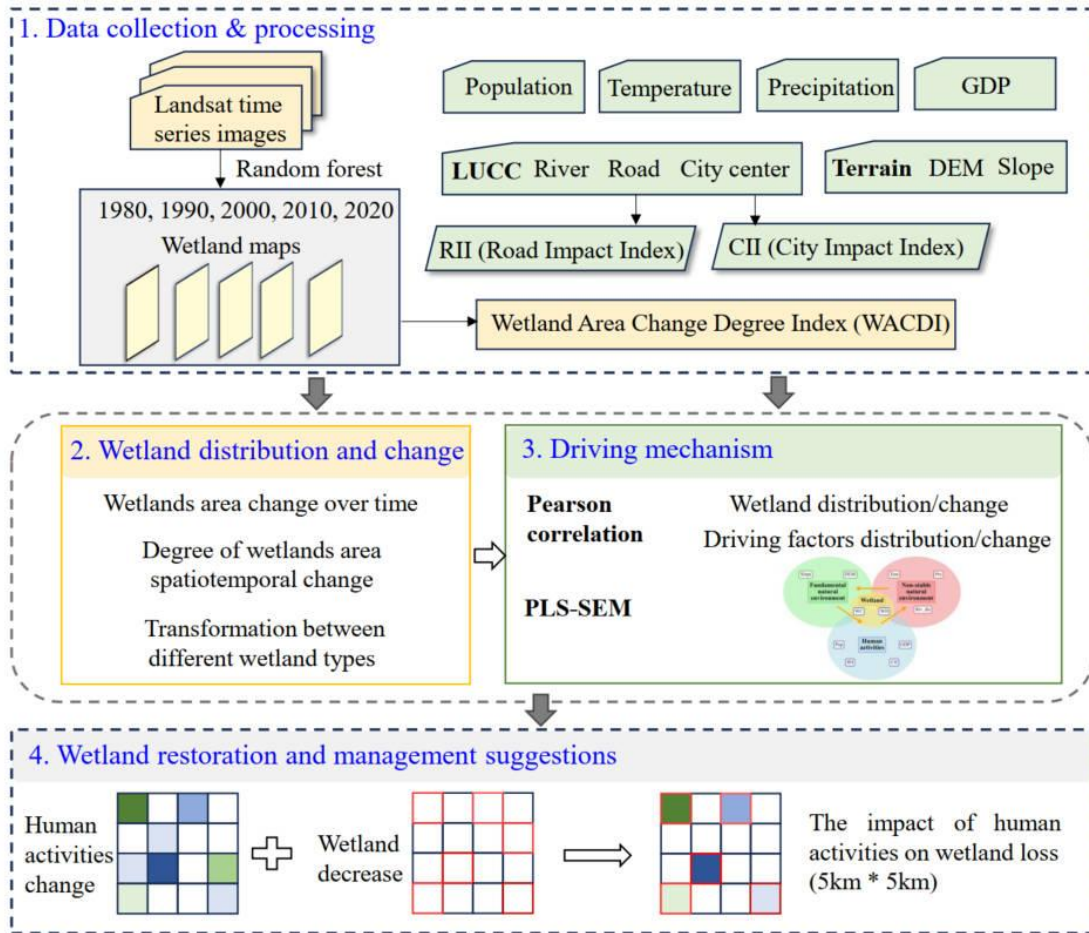


Figure S1 The technical flowchart of this study

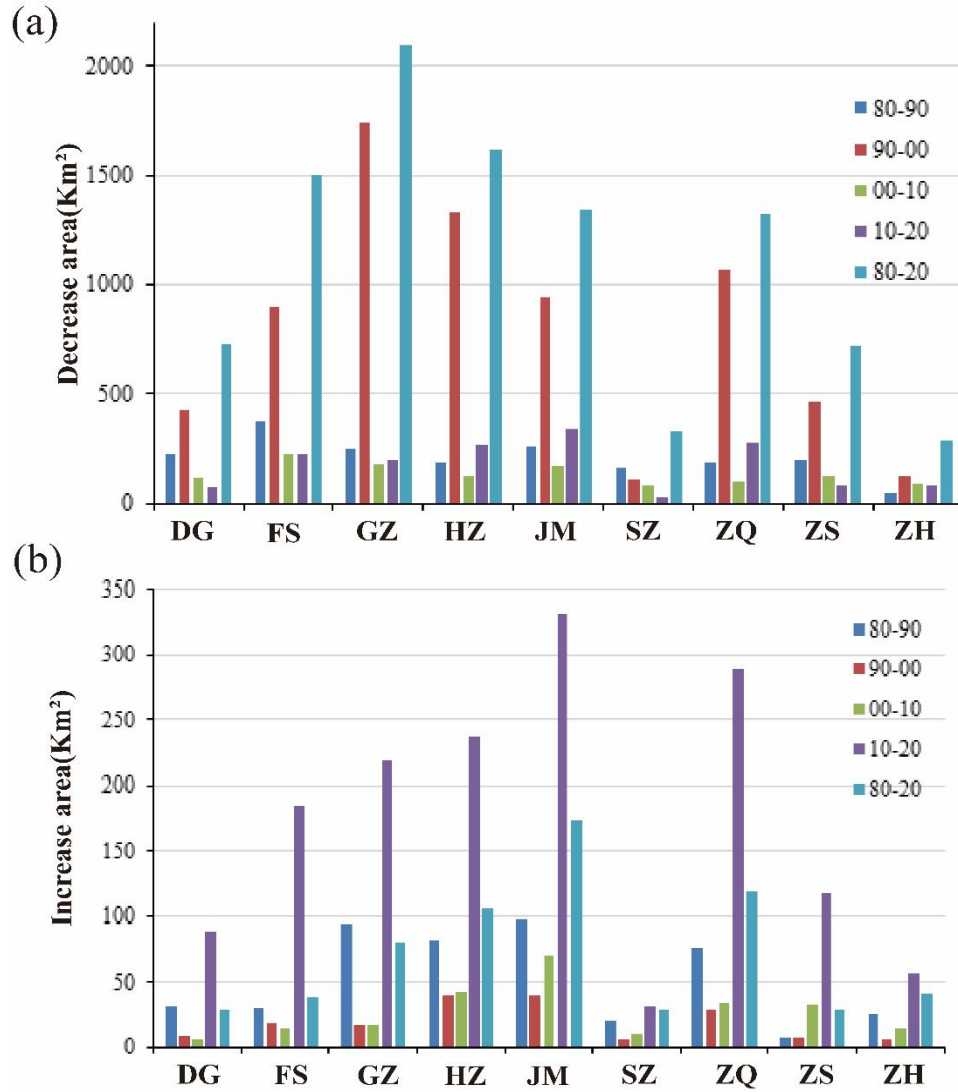


Figure S2. (a) Decreased area and (b) Increased area of wetlands in PRD cities from 1980 to 2020

Table S2. Reliability and validity of PLS-SEM between wetland distribution and driving factors

| Indices | CR | | | AVE | | |
|---------|-------|-------|-------|-------|-------|-------|
| | FNE | NNE | HA | FNE | NNE | HA |
| 1980 | 0.957 | 0.818 | 0.769 | 0.917 | 0.700 | 0.532 |
| 1990 | 0.957 | 0.799 | 0.869 | 0.917 | 0.665 | 0.625 |
| 2000 | 0.957 | 0.844 | 0.879 | 0.918 | 0.731 | 0.644 |
| 2010 | 0.957 | 0.688 | 0.886 | 0.917 | 0.561 | 0.661 |
| 2020 | 0.950 | 0.620 | 0.821 | 0.905 | 0.529 | 0.540 |

Table S3. VIF of PLS-SEM between wetland distribution and driving factors

| Variables | 1980 | 1990 | 2000 | 2010 | 2020 |
|-----------|-------|-------|-------|-------|-------|
| Tem | 1.323 | - | 1.273 | - | 1.070 |
| Pre | 1.323 | 1.122 | 1.273 | 1.042 | 1.070 |
| Slope | 3.312 | 3.296 | 3.330 | 3.302 | 2.919 |
| Dem | 3.312 | 3.296 | 3.330 | 3.302 | 2.919 |
| Riv_dis | - | 1.122 | - | 1.042 | - |
| RII | 1.125 | 1.380 | 1.504 | 1.502 | 1.465 |
| Pop | 1.174 | 5.774 | 6.896 | 1.982 | 5.951 |
| Gdp | - | 5.621 | 6.377 | 3.191 | 5.305 |
| CII | 1.257 | 1.473 | 1.759 | 2.320 | 1.676 |
| Wetland | 1.000 | 1.000 | 1.000 | 1.000 | 1.000 |

Table S4. Reliability and validity of PLS-SEM between wetland increase and changes in driving factors from 2010 to 2020

| Indices | CR | | AVE | |
|-----------|-------|-------|-------|-------|
| | FNE | NNEC | FNE | NNEC |
| 2010-2020 | 0.955 | 0.737 | 0.915 | 0.591 |

Table S5. VIF of PLS-SEM between wetland increase and driving factor changes from 2010 to 2020

| Variables | PreC | Slope | Dem | Riv_disC | CII | WetlandC |
|-----------|-------|-------|-------|----------|-------|----------|
| 2010-2020 | 1.043 | 3.215 | 3.215 | 1.043 | 1.000 | 1.000 |

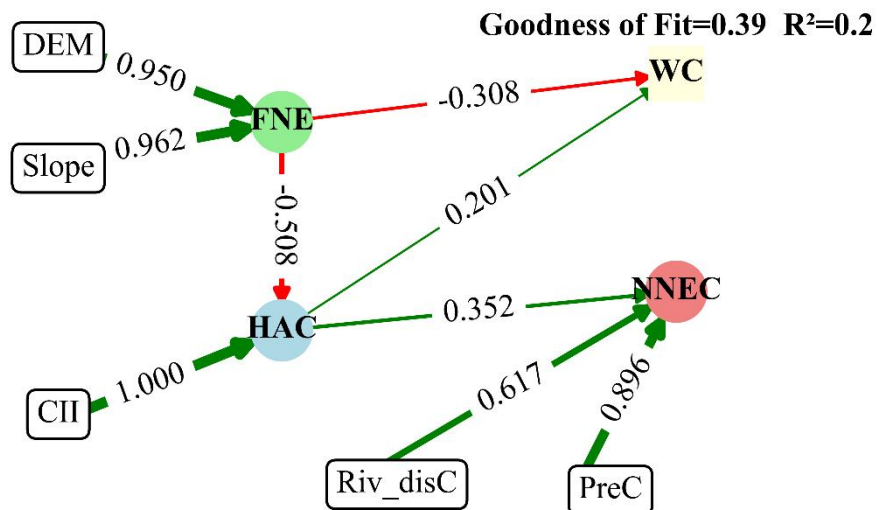


Figure S3. PLS-SEM diagram relationship between each variable and the increase of wetlands during 2010-2020.

Note: The red arrow represents negative impact, while the green arrow represents positive impact. The significance level of all path coefficients is less than 0.001

Table S6. Reliability and validity of PLS-SEM between wetland changes and driving factor changes (wetland decrease from 2010 to 2020)

| Indices | CR | | | AVE | | |
|-----------|-------|-------|-------|-------|-------|-------|
| | FNE | NNEC | HAC | FNE | NNEC | HAC |
| 1980-1990 | 0.957 | - | 0.810 | 0.917 | - | 0.683 |
| 1990-2000 | 0.957 | 0.774 | 0.822 | 0.918 | 0.614 | 0.607 |
| 2000-2010 | 0.957 | 0.789 | 0.781 | 0.918 | 0.575 | 0.547 |
| 2010-2020 | 0.959 | 0.693 | 0.669 | 0.921 | 0.558 | 0.551 |

Table S7. VIF of SEM between wetland changes and driving factor changes (wetland reduction from 2010 to 2020)

| Variables | 1980-1990 | 1990-2000 | 2000-2010 | 2010-2020 |
|-----------|-----------|-----------|-----------|-----------|
| TemC | - | 3.347 | 1.774 | 1.026 |
| PreC | 1.000 | 3.351 | 1.844 | 1.026 |
| Slope | 3.291 | 3.335 | 3.344 | 3.436 |
| Dem | 3.291 | 3.335 | 3.344 | 3.436 |
| Riv_disC | - | 1.004 | 1.054 | - |
| RIIC | - | - | - | - |
| PopC | - | 1.452 | 1.150 | - |
| GdpC | 1.162 | 1.286 | 1.254 | 1.041 |
| CII | 1.162 | 1.337 | 1.233 | 1.041 |
| WetlandC | 1.000 | 1.000 | 1.000 | 1.000 |

Table S8. The direct, indirect and total effects among Fundamental Natural Environment (FNE), Non-stable Natural Environment Change (NNEC), Human Activity Change (HAC) and wetland increase based on the statistically significant SEM paths (2010-2020)

| Path | | | 2010-2020 |
|----------------|----------|--------------|-----------|
| Effect on HAC | Direct | FNE-HAC | -0.508 |
| | Indirect | - | - |
| | Total | FNE~HAC | -0.508 |
| Effect on NNEC | Direct | HAC-NNEC | 0.352 |
| | Indirect | FNE-HAC-NNEC | -0.179 |
| | Total | HAC~NNEC | 0.352 |
| | | FNE~NNEC | -0.179 |
| Effect on WC | Direct | HAC-WC | 0.201 |
| | | FNE-WC | -0.308 |
| | Indirect | FNE-HAC-WC | -0.102 |
| | Total | HAC~WC | 0.201 |
| | | FNE~WC | -0.410 |

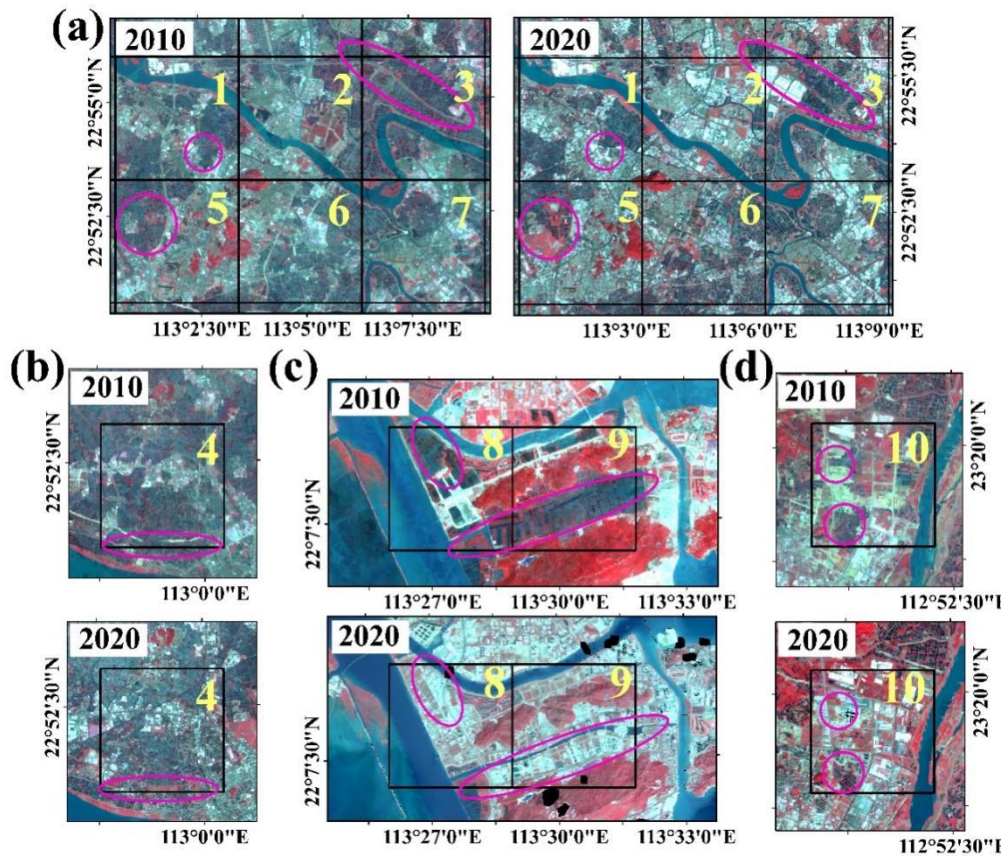


Figure S4. Comparison of typical regional images of human activity changes and wetland loss during 2010-2020 (a) Regions I, 1, 2, 3, 5, 6, 7, (b) Regions I, 4, (c) Regions II, 8, 9 (d) Regions III, 10

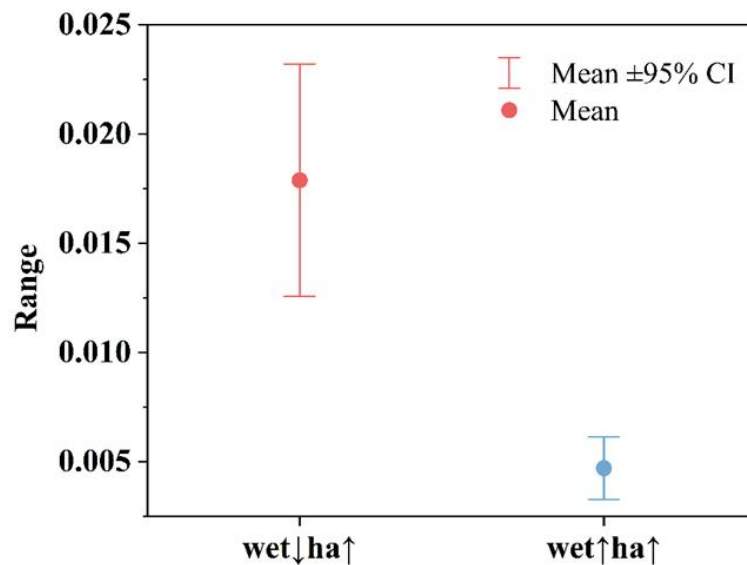


Figure S5. Interval map of human activity range during 2010-2020 estimated by PLS-SEM. Red indicates a decrease in wetland area and an increase in human activity (wet↓ha↑); blue indicates an increase in wetland area and an increase in human activity (wet↑ha↑)